Langmuir and Langmuir-Blodgett films of odorant binding protein/amphiphile study for odorant biosensor

Yanxia Hou, Nicole Jaffrezic-Renault, Claude Martelet, Chaker Tlili, Aidong D. Zhang, Jean-Claude Pernollet, Loïc Briand, Gabriel Gomila, Abdelhamid Errachid, Josep Samitier, et al.

Langmuir and Langmuir-Blodgett films of odorant binding protein/amphiphile study for odorant biosensor

Yanxia Hou [1, 2], Nicole Jaffrezic-Renault [1 ⋆], Claude Martelet [1], Chaker Tlili [1], Aidong Zhang [2], Jean-Claude Pernollet [3], Loïc Briand [3], Gabriel Gomila[4], Abdelhamid Errachid [4], Josep samitier[4], Ludovic Salvagnac [5], Benoit Torbiéro [5], Pierre Temple-Boyer [5]

Centre de Génie Électrique de Lyon (CEGELY), Ecole Centrale de Lyon, 69134 ECULLY Cedex, France
College of Chemistry, Central China Normal University, Wuhan 430079, PR China
INRA, Biochimie et Structure des Protéines, 78325 Jouy-en-Josas, France
Laboratory of NanoBioEngineering, Barcelona Science Park, 08028Barcelona, Spain
5 Laboratoire, d'Analyse et d'Architecture des Systèmes (LAAS) du CNRS, 31077 TOULOUSE Cedex 4, France

Abstract

We have investigated Langmuir and Langmuir-Blodgett films of odorant binding protein/amphiphile for elaboration of artificial olfactory system, namely odorant biosensor. Under optimised experimental conditions the mixed monolayer at air/water interface is very stable and has been transferred efficiently onto functionalised gold supports by SAMs. Electrochemical impedance spectroscopy and atomic force microscopy techniques were used to characterise mixed LB films for detecting one kind of corresponding odorant molecule isoamyl acetate.

Introduction

Many fundamental and central biological recognition and transduction processes occur at biological surfaces. To investigate molecular behaviour of biomolecules at biological surfaces, a well defined and flexible model system is required. Langmuir-Blodgett (LB) films and self-assembled monolayers (SAMs) are believed to be responsible for construction of such model system. LB and SAMs may provide the desired control on the order at the molecular level and thus should be considered desirable techniques for the construction of future organic materials (1).

So far extensive researches have been devoted to either simple systems of Langmuir-Blodgett films (2-4) and self-assembled monolayers (5-7) or complex ones, which combine these two techniques with biocomponents. Particularly interesting, it has been noted that both of these techniques have potential application on elaboration of biosensors. Langmuir-Blodgett technique has already shown its efficiency for depositing well-defined films of enzymes (8-16) and antibodies (17-19) etc. for manufacturing biosensors and it presents numerous advantages such as: rapidity, reproducibility, controlling the amount of the biocomponents and preserving

the activities and specific recognition properties of biomolecules. Since Nuzzo and Allara showed that SAMs of alkanethiolates on gold could be prepared from dilute solutions of dialkyl disulfides (20), the interest in SAMs rapidly expanded and the use of SAMs in various fields of research is rapidly growing. The recent developments show that SAMs play an important role in the construction of biosensors due to its advantages such as simplicity, adaptability, stability and the control over biomolecules surface orientation (21-23).

In this study, we try to elaborate very thin films in which odorant binding proteins (OBPs) were incorporated by the combination of LB films and SAMs; and on the other hand, we hope to perform a preliminary try for an artificial olfactory system, namely, to detect corresponding odorant molecules with such kind of thin films.

Odorant binding proteins, which are abundant low-mol. wt. soluble proteins secreted by the olfactory epithelium in the nasal mucus of vertebrates, play a carrier role for conveying odorants, which are commonly hydrophobic molecules, to their neuronal receptors through nasal mucus (24). In present report a novel rat odorant-binding protein variant OBP-1F was used for the preparation of mixed protein/amphiphile LB films. The experiments were performed in the subphase of phosphate buffer solution (PBS) at a pH of 7.5. Under the condition, OBP-1F is perfectly soluble and active. Fatty amine octadecylamine (ODA) was chose as amphiphile taking into account of the fact that at such a pH OBP-1F could be considerably better adsorbed onto positively charged lipid monolayers such as amine than neutral or negatively charged ones. Since the pK_a of OBP-1F is 5.20, the protein molecules are mainly negatively charged at the pH of 7.5. In addition, the use of fatty amines will allow us to carry out a crossing-linking step between amine terminal moieties (coming from protein and fatty amine) and crossing-linking reagent glutaraldehyde molecules in order to improve the stability of the transferred LB films as reported by Sun (9) and Chovelon (15). Furthermore, the presence of the protein and counter-ions of hydrogen phosphate (25) in the subphase were expected to be favourable for stability of fatty amine monolayer at air/water interface.

It's known that the basic LB technique consists in elaborating a monolayer of the amphiphile molecules on the subphase containing soluble protein and then transferring the monolayer onto the solid substrates by vertical dipping procedure (Langmuir-Blodgett) or horizontal one (Langmuir-Schfäer). For obtaining high-quality LB films the properties of the monolayer especially stability was investigated here, since it plays a key role in obtaining stable and reproducible LB film, which is essential for biosensor application. And LB films of odorant binding protein/amphiphile, OBP-1F/ODA in our case, were deposited by most often used vertical dipping procedure onto gold substrates, which were functionalised with 1-

octadecanethiol by SAMs to provide a biomimetic and hydrophobic surface favourable for the deposition of OBP-1F/ODA LB films.

Such mixed LB films system, on the one hand, may constitute interesting models for biological membranes and structures, may be used for studying and testing isolated functions; on the other hand, such structures may be used for designing artificial systems inspired by biological structures or functions and possessing analogous properties. Consequently, the obtained LB films were exposed to one of corresponding odorant molecule for elaboration of odorant biosensor.

In this study several techniques including scanning electron microscopy (SEM), atomic force microscopy (AFM) and electrochemical impedance spectroscopy (EIS) have been applied to characterise LB films for odorant biosensor. AFM is considered a powerful tool in microbiology (26-27) and it is also an interesting tool for the characterization of LB films (10, 16, 28-29) in that it could give access to the molecular architecture. And a complementary technique EIS is a rapidly developing electrochemical technique for the characterization of biomaterial-functionalised electrode surface and has potential application on biosensor, since it represents not only a suitable transduction technique to follow the interfacial interactions of biomolecules, but it also provides a very powerful method for the characterization of the structural features of the sensing interface and for explaining mechanisms of chemical processes occurring at the electrode/solution interface(30-32). The results obtained from AFM and EIS have been discussed.

Materials and Methods

2.1. Materials

OBP-1F (wt 18 538 Da) and its corresponding odorant molecule isoamyl acetate were both provided by Laboratory of Biochemistry and Structure of Proteins, INRA, France, and were used without any further purification. Octadecylamine (ODA) (purity > 99%) and 1-octadecanethiol (ODT) (purity 98%) were purchased from Fluka and Aldrich Chemical Company, respectively. Solvent chloroform (purity 99.8%) bought from Aldrich Chemical Company was applied for dissolving ODA at a concentration of 1 mg/ml. And ODT was dissolved at a concentration of 1 mM in ethanol (purity > 99.8%) obtained from Fluka for modification of gold substrate. Potassium dihydrogen phosphate, sodium chloride both from PROLABO, and sodium hydroxide from Aldrich Chemical Company were used to prepare 10 mM phosphate buffer solution (consisting of 100 mM NaCl, pH 7.5), which was used for both

LB films preparation and impedance measurements. And all of them are analytical grade reagents (>99%).

In present study, OBP-1F solutions were prepared freshly on the day of experiment by dissolving the protein in PBS (pH 7.5). Water used through all experiments was purified by an Elga system with a reverse osmosis, deionization, filtration and ultraviolet irradiation systems to have a resistance as high as 18.2 mΩ.cm. Its pH was about 5.5, and its surface tension was 71.8 $mN.m^{-1}$ at 25 °C in air.

And all glassware that was to come into contact with the samples, solutions, or solvents was washed well with sulfochromic solution, rinsed with copious amounts of ultrapure water and then acetone, dried for overnight in a sealed oven at 100 °C.

2.2. Gold substrate and monolayer preparation

Gold substrates were fabricated using standard silicon technologies. <100>-oriented, P-type (3-5 Ω.cm) silicon wafers were thermally oxidised to grow a 800nm-thick field oxide. Then, a 30nm-thick titanium layer and a 300nm-thick gold layer were deposited by evaporation on top. The formation of a monolayer on gold is strongly dependent on several factors, such as the cleanliness and structure of gold prior to modification. As known gold is a soft metal and is readily contaminated by organic and inorganic species during manual handling (33). Consequently, the fabrication process and the pre-treatment, namely cleanliness, of gold substrates are considered very important.

In present study, the whole metallization process was optimised in order to keep a good adherence of the Ti/Au layer on the field oxide which reaching good properties of the gold upper surface. This optimisation has lead to the use of low deposition rates (around 1 nm/s) for both evaporation processes and to the suppression of the Ti/Au annealing process (250°C – 20 min). In the same way, the cleaning procedure has been optimised as follows. The gold substrates were previously cleaned with acetone in an ultrasonic bath for 10 min and dried under a nitrogen flow, followed by immersion in 7:3 (v/v) H_2SO_4:H_2O_2 (piranha solution) for 1 min in order to get rid of inorganic and organic contaminants on the substrate surface. (Caution: piranha solution reacts violently with organic materials and should be handled very carefully.) They were subsequently rinsed thoroughly in absolute ethanol and finally dried under a N_2 flow.

As soon as the cleaning procedure terminated, the substrates were put into 1 mM ODT solution for 21 h at room temperature to make their surfaces hydrophobic by the formation of

SAMs. Excess thiol was removed from the surface by rinsing thoroughly the substrates with ethanol and finally substrates were dried under a N_2 flow.

A contact angle meter (GBX scientific instruments, France) was utilised to measure the contact angle of gold surface. We found that the contact angle of the as-received gold substrate is 50° due to the presence of organic contaminant layer (34). However, after cleaning the substrates were hydrophilic with contact angle < 10° attributed to an organic contaminant-free surface, and they were hydrophobic after formation of well-ordered SAMs with contact angle 110° ± 3°.

2.3. Langmuir and Langmuir-Blodgett films

Langmuir experiments were performed with a Langmuir trough from NIMA (model 611) with an effective surface 30 cm × 10 cm and the volume of the liquid phase 200 ml. Moreover, this system consists of two mobile barriers for compressing amphiphilic monolayer and a Wilhelmy balance which was equipped with a strip of chromatography paper suspended at the air-water interface for measuring interfacial pressure. The trough is equipped with a chamber for preventing external contamination.

The subphase temperature was controlled at 10 ± 1 °C by a thermostatic system (Julabo-F25, France). The subphase was constituted of solution of OBP-1F in PBS at different concentration or in ultrapure water. Before each experiment, the surface of the subphase was cleaned by aspiration. And the surface was considered clean when the change in surface pressure of the subphase upon compression of the area was smaller than 0.1 mN m^{-1}.

For elaboration of mixed layer of octadecylamine and protein OBP-1F, the protein solution in PBS was used as subphase and 22 µL ODA in chloroform was injected and spread onto interface by a micropipette of 50 µL. It was spread from the same distance above the subphase in all the experiments. After spreading, the monolayers were left for at least 15 min to allow the solvent to evaporate. Proteins were allowed to adsorb from the subphase to the air/water interface for about 3 h. The apparent molecular area was defined as the ratio of the film area to the number of ODA molecules. Then the compression of the film was initiated at a rate of 5 cm^2 min^{-1} until the target surface pressure was reached. Relaxation time of 3 h was required before onset of dipping. While the surface pressure was kept constant and the monolayer was stable, the monolayer was transferred onto hydrophobic gold substrates by vertical dipping method at a rate of 3 mm min^{-1}. After each upstroke, the substrate was maintained in air for 5 min to dry the films. The transfer ratio (TR) expressed as the ratio of area of film transferred

onto the monolayer-coated area on the substrates was used as a parameter to characterize LB deposition. After transfer of LB films functionalized gold substrates were put into the vapour of glutaraldehyde for 15 min, in order to stabilize LB layers by cross-linking with this bifunctional reagent. Then they were used for the following experiments.

For understanding well formation of Langmuir and Langmuir-Blodgett films, first we have studied the properties of monolayer at air/water interface. For studying adsorption of protein to amphiphile monolayer at the air/water interface, surface pressure-time curves (referred to as π -t) were recorded with opened barrier, namely without compressing force. The characteristics of the monolayer on the surface were studied by measuring the changes in surface pressure upon compressing the monolayer at a given temperature, namely surface pressure-molecular area isotherm (referred to as π -A). The shape of the isotherm is characteristic of the molecules making up the film. The stability of the monolayer, which is an important parameter for the stability of the mixed LB films, can be demonstrated by molecular area ratio-time evolution isotherms at the target pressure (referred to as A/A_0-t) or surface pressure-time evolution at a constant molecular area (referred to as P_b-t).

2.4. Volatile-odorant binding

After the deposition and stabilization of OBP-1F/ODALB films the substrates were put in a 2-L sealed glass chamber containing pure undiluted odorant isoamyl acetate (10 μL in the chamber) which evaporated freely for 16 h at room temperature. And the samples were then used for AFM and EIS measurements.

2.5. Langmuir-Blodgett films characterization

2.5.1. Scanning Electron Microscopy

SEM images were taken using a scanning electron microscope (Philips XL20). The accelerating voltage was 10 kV.

2.5.1. Atomic Force Microscopy

Atomic force microscopy measurements were obtained in air at room temperature using a Pico+ Microscope (Molecular Imaging). Tapping mode was used to avoid damaging the surface of the sample. Silicon rectangular cantilevers (NCL, Nanoworld) with normal spring constant of 48 N/m and resonance frequency of 190 kHz were used (typical curvature radius of the tip 10 nm).

2.5.2. Electrochemical Impedance Spectroscopy

Impedance measurements were performed in a conventional electrochemical cell containing a three-electrode system with an Electrochemical Interface SI 1287 and a Frequency Response

Analyser 1255B from Solartron. A Pt plate and a saturated calomel electrode (SCE) were used as counter and reference electrode, respectively. And gold substrates with LB films deposition were working electrodes with effective surface 0.07 cm^2. Impedance measurements were taken in absence of any redox probe in PBS at ambient temperature and in the frequency range from 50 mHz to 100 kHz, at the formal potential of –600 mV using alternate voltage of 10 mV.

Results and discussion

3.1. Adsorption of protein at air/water interface

The surface pressure vs time (π-t) curves presented in Figure1. were measured for the adsorption of protein at air/water interface at three different protein concentrations: 4, 6 and 10 mg L^{-1}. And they were collected without compressing force.

It can be seen from the Figure1 increase of the surface pressure was strongly dependent on concentration of protein in the subphase and time. The higher concentration of protein OBP-1F, the higher surface pressure. It is in accordance with the kinetics of adsorption, for higher protein concentration, more protein molecules went up towards interface under the same adsorption time. In addition, from the figure we can find the surface pressure increases rapidly at the beginning and continues to increase but slowly after 250 min, which means there are still more protein molecules which are prone to penetrate lipid layers and adsorb at air/water interface. However, it took even more than 10 hours to reach adsorption equilibrium. Considering the fact that such a long adsorption time may result in evaporation of water in the subphase, and thereby may produce some unfavourable effect on accuracy of the experimental results, proteins were allowed to adsorb from the subphase for about 3 h.

Curiously, comparing to the results of adsorption of protein Butyrylcholinesterase (BuChE) at air/water interface studied by Chovelon et al. (15), we found that the surface pressure in the case of OBP-1F is comparatively low. For example, at the protein concentration 4 mg L^{-1} for both of cases, the surface pressure is approximately 25 mN m^{-1} for BuChE with adsorption time 250 min, but only about 11 mN m^{-1} for OBP-1F.

Proteins follow a diffusion-controlled adsorption mechanism at air/water interface. They are prone to penetrate lipid layer and expose the hydrophobic part upon the air phase at air/water interface, which can proceed as long and as far as there is time and space at the interface available (35). Still more in the presence of ionic surfactant, such as ODA in this study, proteins can be adsorbed onto or between head of amphiphile molecules by electrostatic interaction. At low surface pressure while without compressing force, the diffusion-controlled adsorption plays a predominant role on increment of surface pressure. However, it’s reported that the rate of

desorption of proteins increases markedly with decreasing molecular weight at a given surface pressure (36). Consequently it's evident that surface pressure for BuChE (wt 444 000Da) is higher than that for OBP-1F (18 538Da). At low surface pressure, molecules of BuChE are more prone to spread at air/water interface. However for ODA-1F the rate of desorption of protein OBP-1F is so high in the subphase that the increase of surface pressure arises mainly from the adsorption of protein to amphiphile molecules.

3.2. Surface pressure-molecular area isotherms

Three different subphases: ultrapure water, PBS at pH 7.5 without and with OBP-1F were used to investigate the characteristics of the corresponding amphiphile monolayers. The surface pressure –molecular area isotherms of amphiphile molecules on ultrapure water were considered as a reference. For the mixed film, an apparent molecular area was defined as the ratio of the film area to the number of amphiphile molecules.

We can see from the Figure 2 ingredient in the subphase has apparent influence on the characteristics of the amphiphile monolayers at the air/water interface. For ultrapure water as subphase, extrapolated to 0 mN m^{-1} from the linear portion of the compression curve gives an apparent surface area of only15 $Å^2$/ODA, which is lower than the theoretical value of 21 $Å^2$/ODA. It results most likely from dissolution of one small part of ODA molecules in the water , which demonstrates the ODA monolayer at air/water interface is not very stable with ultrapure water as subphase.

However, for PBS as subphase the curve is considerably different from that with ultrapure water as subphase. We can see from Figure 2 at low surface pressure the molecular area of the ODA monolayer with the PBS as subphase was much larger than that of the ODA monolayer in ultrapure water. It is proposed that at the pH 7.5, the amino head of ODA should be positively charged, the addition of strongly bound multivalent counter-ions, such as PO_4^{3-} in the PBS subphase have effect on the monolayer. Perhaps at low surface pressure aggregate of long-chain amine ODA around PO_4^{3-} took place. On the other hand, extrapolated to 0 mN m^{-1} from the linear portion of the compression curve gives an apparent surface area of 20 $Å^2$/ODA, which is very close to the theoretical value. We can conclude there is nearly no dissolution of ODA molecules under such condition. The increased stability of the monolayer as expected is attributed to the addition of counter ions in the subphase, which induced interaction between anions and positively charged amines.

In the case of PBS subphase with protein OBP-1F, the molecular area is still greater than without OBP-1F at low surface pressure, it means that interaction exists also between protein and ODA molecules, and some of protein molecules were inserted into the ODA monolayer.

As referred above while surface pressure lower than 10 mN m^{-1}, protein not only can penetrate amphiphile monolayer and spread at air/water interface by diffusion, but also can be adsorbed onto or between head of amphiphile molecules by electrostatic interaction. And then with compression the increase of surface pressure leads to approach of protein and amphiphile molecules until phase transition of the monolayer from liquid to solid, between 30 and 40 mN m^{-1} in the Figure 2, in which a slight increase of the surface pressure is observed with the molecular area decreasing. Since protein molecules which spread at air/water interface are gradually expelled from the interface and pushed under the positively charged head of ODA molecules. As a consequence the surface pressure does not increase significantly. More importantly, in this range of surface pressure the monolayer includes a relative high amount of protein and it's desirable for the formation of Langmuir-Blodgett films and elaboration of biosensors. Since with the further compression, surface pressure above 40 mN m^{-1} in the figure, there is risk of overlapping of monolayer and even worse completely collapsing of the monolayer.

In the following study we investigated the stabilities of the monolayers in the transition state and tried to obtain the optimal target pressure for deposition of LB films.

3.3. The stability of the mixed protein/amphiphile monolayer

The stability of the mixed monolayer is very important because it is related to the transfer efficiency and the quality of deposited LB films. It can be examined by the evolution of surface pressure with time at a fixed molecular area, or the evolution of molecular area ratio with time at a fixed surface pressure, after the monolayer has been compressed.

As has been reported by our group (14), the pure amphiphile monolayer is unstable because of its partial solubility in the subphase. However, we can see from Figure 3 monolayers with different surface pressures (30, 35, 40, 43 mN m^{-1}) and from Figure 4 monolayers with different concentration (4, 6, 10 mg L^{-1}) of the proteins are all very stable. This confirms that the addition of protein in the subphase increases indeed the stability of the monolayer at air/water interface. In fact, as has been referred by Miller (35) electrostatic interaction between protein and surfactant such as amphiphile induce formation of protein/surfactant complex which is much less soluble than the protein and also have the highest surface activity.

Another phenomenon can be seen from the figures is that the surface area of monolayer decreases quickly at the beginning and then decreases much more slowly with time. This initial loss in area depends on the rate at which the monolayer is compressed and is due to a structural rearrangement occurring within the layer. Meanwhile, the very slight decrease with time is likely result from the feeble solubilization of the mixed monolayer.

3.4. Transfer of Langmuir-Blodgett films

The stable mixed protein/amphiphile monolayer has been transferred from air/water interface onto solid substrates of gold under different target pressures (30, 35, 40, 43 mN m^{-1}). Since the gold substrates have been functionalised with SAMs of ODT to be hydrophobic, deposition of LB films should occur during the first downstroke of the substrate through air/water interface.

We found for target pressure 35 mN m^{-1}, LB films can be transferred successfully onto gold substrates with good reproducibility and very high transfer ratio as shown in Figure 5, which corresponds to a Y-type deposition. Furthermore, it can be seen from Figure 4 that at target pressure (35 mN m^{-1}) the stabilities of the monolayers seem have nothing to do with the concentration of protein, which is consistent with the fact that at this surface pressure the proteins were thoroughly expelled from the interface and were adsorbed onto the ODA monolayer. As a consequence, it has been chosen as target pressure for the following studies of AFM and EIS.

Scanning electron microscopy (SEM) was used to characterize LB films obtained at different target pressures at a submillimeter scale in order to obtain some general topographic information. As is shown in Figure 6 the structures appear to be heterogeneous with protein aggregates being dispersed at random on the samples and many defects presenting. The important rearrangements probably occur during and/or after the transfer. This kind of structure of LB films has been reported by Sommer et al. (29) and Chevelon et al. (16) with AFM. However, we could not identify the chemical nature of the different structures obtained by SEM.

In addition, by comparing the four images, we found that at higher surface pressure, in the cases of surface pressure 40 and 43 mN m^{-1}, the structures of LB films on the gold substrates seem to be more homogeneous, and protein aggregates approach more and more each other. However, we found that under these high surface pressures, the transfer of LB films were not so effective. We think at the surface pressure 40 and 43 mN m^{-1}, the phase transition of the monolayer from liquid to solid nearly terminates, the molecules are closely packed. In this

state, the monolayer is much more sensitive and fragile to any external force, it's reasonable to assume the vertical passage of the solid substrate could damage probably the monolayer, resulting in overlapping or partly collapsing of the monolayer. And consequently the transfer ratios for LB films at these surface pressures are lower.

3.5. Characterization of Langmuir-Blodgett (LB) films for odorant biosensor

3.5.1. Electrochemical impedance spectroscopy (EIS) (Reference 37 38)

After two layers of mixed OBP-1F/ODA LB films were efficiently transferred onto functionalized gold substrates at 35 mN m^{-1}, an EIS measurement was employed to characterize such structures (gold/thiol/ODA/OBP LB films) before and after exposure to odorant molecules isoamyl acetate, since EIS is an effective method to investigate the interface properties of an electrode.

The magnitude (|Z|) and the phase angle theta *versus* frequency (Figure 7a and b, respectively) show the behaviour over the entire frequency range, while the linear Nyquist plot (Figure 7c) more clearly emphasizes the impedance changes at low frequency where the experimental results show best sensitivity to odorant molecules.

An understanding of the physical origin of the observed response can be enhanced using electrical circuit modelling, in which the electrical response of the physical interface is modelled using various discrete electrical circuit elements. However, no equivalent model can be guaranteed to be unique. The model that provides best fit to the data over the entire frequency range in our study is shown in Figure 7d. And the interpretation for each electrical circuit element (R_s, R_{SAMs}, C_{SAMs}, R_{LB}, Q_{LB}) is described as follows:

R_s is solution resistance;

R_{SAMs}

C_{SAMs}

R_{LB}

Q_{LB}

At frequencies below A, the total impedance is dominated by the OBP-1F/ODA LB film and the impedance of Q_{LB}. At intermediate frequencies (between A and B) the impedance is dominately mainly by the C_{SAMs}, which has no significant sensitivity to binding of odorant molecules. At the highest frequencies (greater than B) the impedance is mainly dependent on the bulk solution resistance, R_s, which is dependent upon the ionic strength of the buffer that is used.

Probably the binding of odorant molecules induced the rearrangement of the mixed OBP-1F/ODA LB film and/or local conformational change of OBP molecules.

The binding of ligand was shown to induce local conformational changes. The arrangement is therefore possible, leading to favourable contact between, a local conformational transition upon binding . It has been proved that OBP-1F undergoes a conformational change upon odorant binding (24). Odorant binding proteins share a conserved folding pattern, an eight-stranded β-barrel flanked by an α-helix at the C-terminal end of the polypeptide chain. The β-barrel defines a central apolar cavity, called the calyx, whose role would be to bind and transport hydrophobic odorant molecules.

3.5.2. Atomic force microscopy (AFM)

Topographic images of the mixed OBP-1F/ODA LB films remain almost unchanged at the scale of the figures (10nm) after exposure to odorant. However we have identified a strong change in the AFM phase images after exposure to the odorant, see Figure 8. The white spots in topographic images are probably dust or salts remaining after the rinsing process.

Indeed, before exposure to the odorant phase is almost uniform on the sample (variations of maximum of ~1º are observed), after exposure to the odorant a big contrast is observed between the aggregates and the rest of the sample, with phase variations of up to ~9º. Since phase atomic force microscopy images, by recording the phase lag existing between the signal that drives the cantilever and the cantilever oscillation output signal, provides information about surface properties such as elasticity, adhesion and friction, we can conclude that a modification in one (or all) of these mechanical properties has occurred on the aggregates. An obvious possibility would be to assume that the aggregates being more rich in OBPs have captured far more odorant molecules than the surrounding regions, thus changing the adhesion force of the tip on these regions. While this is a very reasonable possibility, that would confirm the EIS data, it seems difficult to correlate the observed changes with a possible molecular arrangement of the proteins since a lot of arrangements in this case are possible (16). Direct topographic information on the conformational changes would require almost atomic resolution that can not be achieved under the present experimental conditions.

4. Conclusion

In this paper, we have carefully studied both odorant binding protein/amphiphile Langmuir and Langmuir-Blodgett films and we have shown that stable mixed Langmuir films can form at air/water interface as well as can be efficiently transferred onto gold supports at target pressure 35 mN m^{-1} for construction of reproducible and stable mixed LB films. Such kind of thin films exhibits desirable application on elaboration of artificial olfactory system. With EIS and AFM techniques we found that such system can detect corresponding odorant molecules. (need more results and information from EIS and AFM)In further study we expect to produce sensor array for fabricating electronic nose based on this kind of mixed LB films and to detect a series of airborne odorants not only one.

Acknowledgements

This work was financially supported by Concerted Action NMAC (N_0 0220306) and the SPOT-NOSED Project (IST-2001-38739).

Reference

(1) Ulman, A. An Introduction to Ultrathin Organic Films: From Langmuir-Blodgett to Self-Assembly; Academic Press; Boston, 1991

(2) Petty, M. C. Langmuir-Blodgett films: An introduction; Cambridge University Press; 1996

(3) Bardosova, M.; Tredgold, R. H.; Ali-Adib, Z. Langmuir 1995, 11, 1273-1276

(4) Datta, A.; Kmetko, J.; Yu, C.; Richter, A. G.; Chung, K.; Bai, J. and Dutta, P. J. Phys. Chem. B 2000, 104, 5797-5802

(5) Ulman, A. Chem. Rev. 1996, 96, 1533-1554

(6) Schoenfisch, M. H., and Pemberton, J. E. J. Am. Chem. Soc. 1998, 120, 4502-4513.

(7) Laibinis, P. E., Whitesides, G. M., Allara, D. L., Tao, Y., Parikh A. N., and Nuzzo,R. G. J. Am. Chem. Soc. 1991, 113, 7152-7167.

(8) Okahata, Y.; Tsuruta, T.; Ijiro, K.; Ariga, K. Langmuir 1988, 4, 1373-1375

(9) Sun, S.; Ho-Si, P. H.; Harrison, D. J. Langmuir 1991, 7, 727-737

(10) Dubreuil, N.; Alexandre, S.; Fiol, C.; Sommer, F. and Valleton, J. M. Langmuir 1995, 11, 2098-2102

(11) Girard-Egrot, A.P.; Morélis, R.M.; Coulet, P.R. Langmuir 1997, 13, 6540-6546

(12) Rosilio, V.; Boissonnade, M. M.; Zhang, J.; Jiang, L. and Baszkin, A. Langmuir 1997, 13, 4669-4675

(13) Fiol, C. ; Valleton, J. M.; Delpire, N.; Barbey, G. ; Barraud, A. and Ruaudel-Teixier, A. Thin Solid Films 1992, 210/211, 489-491

(14) Zhang, A.; Jaffrezic-Renault, N. Wan, J.; Hou, Y. and Chovelon, J. M. Materials Science and Engineering C 2002, 21, 91-96

(15) Chovelon, J. M.; Wan, K.; and Jaffrezic-Renault, N. Langmuir 2000, 16, 6223-6227

(16) Chovelon, J. M.; Gaillard, F.; Wan, K.; and Jaffrezic-Renault, N. Langmuir 2000, 16, 6228-6232

(17) Tronin, A.; Dubrovsky, T; Nicolini, C. Thin Solid Films 1996, 284/285, 894-897

(18) Vikholm, I.; Teleman, O., Journal of Colloid and Interface Science 1994, 168, 125-129

(19) Barraud, A., Perrot, H., Billard, V., Martelet, C., Therasse, J., Biosensors and Bioelectronics 1993, 8, 39-48

(20) Nuzzo, R. G.; Allara, D. L. J. Am. Chem. Soc. 1983, 105, 4481-4483

(21) Wink, T.; Zuilen, S. J. V.; Bult, A.; Bennekom, W. P. V. Analyst 1997, 122, 43R-50R

(22) Ferretti, S.; Paynter, S.; Russell, D. A.; Sapsford, K. E. Trends in Analytical Chemistry 2000, 19, 530-540

(23) Spinke, J.; Liley, M.; Guder, H. J.; Angermaier, L. and Knoll W. Langmuir 1993, 9, 1821 - 1825

(24) Nespoulous, C.; Briand, L.; Delage, M. M.; Tran, V. and Pernollet, J.C. Chem. Senses 2004 29, 189-198

(25) Gains, G. L. Jr Nature 1982, 298, 544-545

(26) Dufrêne, Y. F. Journal of Bacteriology 2002, 184, 5205-5213

(27) Fotiadis, D. ; Scheuring, S. ; Müller, S. A.; Engel, A. and Müller, D. J. Micron 2002, 33, 385-397

(28) Fujiwara, I.; Ohnishi, M.; and Seto, J. Langmuir 1992, 8, 2219-2222

(29) Sommer, F. ; Alexandre, S. ; Dubreuil, N. ; Lair, D. ; Tran-minh Duc, and Valleton, J. M. Langmuir 1997, 13, 791-795

(30) Katz, E.; Willner, I. Electroanalysis 2003, 15, 913-947

(31) Hou, Y.; Tlili, C.; Jaffrezic-Renault, N.; Zhang, A.; Martelet, C.; Ponsonnet, L.; Errachid, A.; samitier, J.; Bausells, J. Biosensors and Bioelectronics, accepted.

(32) Janata, J. Critical Reviews in Analytical Chemistry 2002, 32, 109-120

(33) Yang, Z.; Gonzalez-Cortes, A.; Jourquin, G.; Viré, J. C.; Kauffmann, J. M. ; Delplancke, J. L. Biosensors and Bioelectronics 1995, 10, 789-795

(34) Ron, H.; Matlis, S.; Makievski, A. V.; Krägel, J.; Grigoriev, D. O.; Kazakov, V. N.; Sinyachenko, O. V. Advances Rubinstein, I. Langmuir 1998, 14, 1116-1121

(35) Miller, R.; Fainerman, V.B.; in Colloid and Interface Science 2000, 86, 39-82

(36) Dziri, L.; Puppala, K. and Leblanc, R. M. Journal of Colloid and Interface Science 1997, 194, 37-43

(37) Lasseter, T.L.; Cai W. and Hamers, R.J. Analyst 2004, 129, 3-8

(38) Briand, L.; Nespoulous, C.; Perez, V.; Rémy, J. J.; Huet, J. C. and Pernollet, J. C. Eur. J. Biochem. 2000, 267, 3079-3089

Figure captions

Figure 1. Adsorption of OBP-1F at the air/water interface as a function of time.

Figure 2. Surface pressure-area isotherms for amphiphile ODA with different subphases: water, phosphate buffer solution (10 mM, pH 7.5) without and with protein OBP-1F (4 mg L^{-1}).

Figure 3. Evolution of the molecular area for the mixed monolayer at constant surface pressures of 30, 35, 40, 43 mN m^{-1} (protein concentration 4 mg L^{-1}).

Figure 4. Evolution of the surface pressure for the mixed monolayer at constant molecular area for the different concentrations of protein 4, 6, 10 mg L^{-1}.

Figure 5. Transfer ratio for 2 mixed proteinOBP-1F/ODA LB films deposition at target pressure 35 mN m^{-1}.

Figure 6. SEM images of two layers of mixed OBP-1F/ODA LB films transferred onto gold substrates at (a) 30 mN m^{-1}, (b) 35 mN m^{-1}, (c) 40 mN m^{-1} and 43 mN m^{-1}.

Figure 7. Bode diagrams are shown in (a) the magnitude (|Z|) *versus* frequency and (b) the phase angle theta *versus* frequency, in which the symbols represent experimental values and the straight lines represent fitting data: (□) before exposure to odorant molecules, (○) after exposure to odorant molecules. (c) Nyquist (Z" vs. Z') plots measured for gold/thiol/ODA/OBP LB films before (A) and after (B) exposure to odorant molecules. (d) The equivalent circuit model used to fit the impedance data, the electrical circuit elements were described in the text.

Figure 8. AFM Topographic (a) and phase (a') images of a mixed ODA/OBP LB film transferred onto functionalized gold substrate at 35 mN m^{-1} before exposure to odorant. Scan area 2.1x2.1 □m^2. Vertical scale (a) 10 nm, (a') 1.3º. AFM Topographic (b) and phase (b') images of a mixed ODA/OBP LB film transferred onto functionalized gold substrate at 35 mN m^{-1} after exposure to odorant. Scan area 4x4 □m^2. Vertical scale (b) 10 nm, (b') 9.4º.

Table.1. Values of circuit elements in the equivalent circuit obtained by fitting the experimental data from Figure 7c to the circuit model shown in Figure 7d.

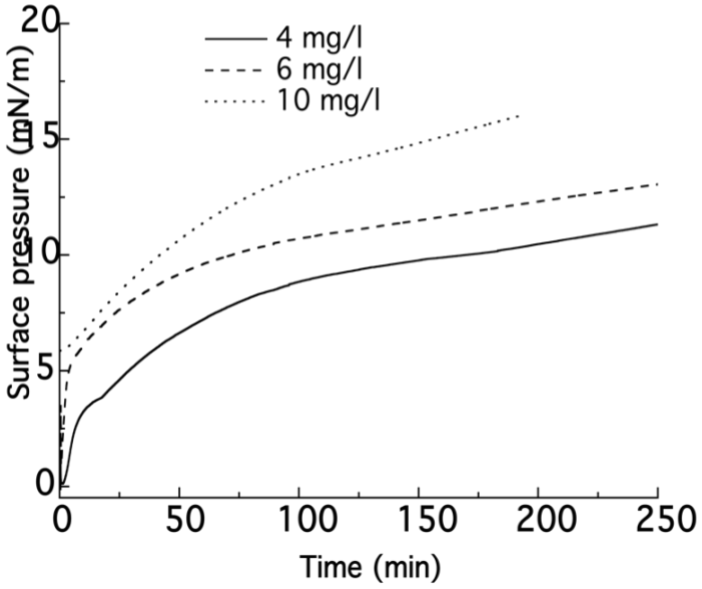

Figure 1.

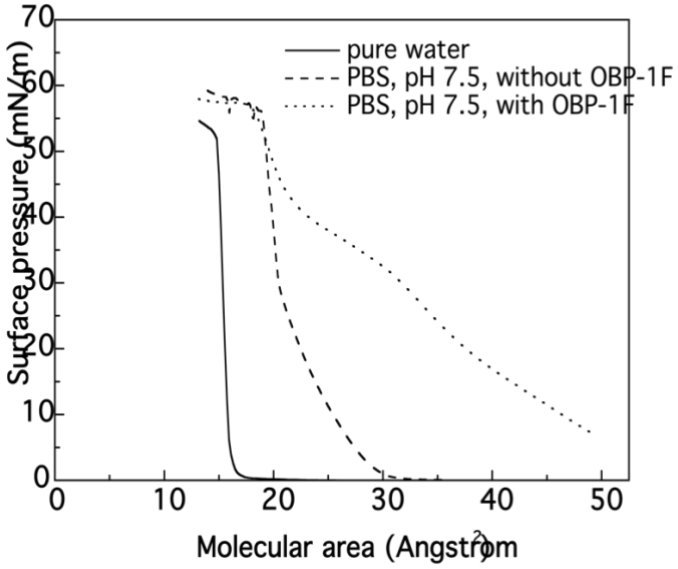

Figure 2.

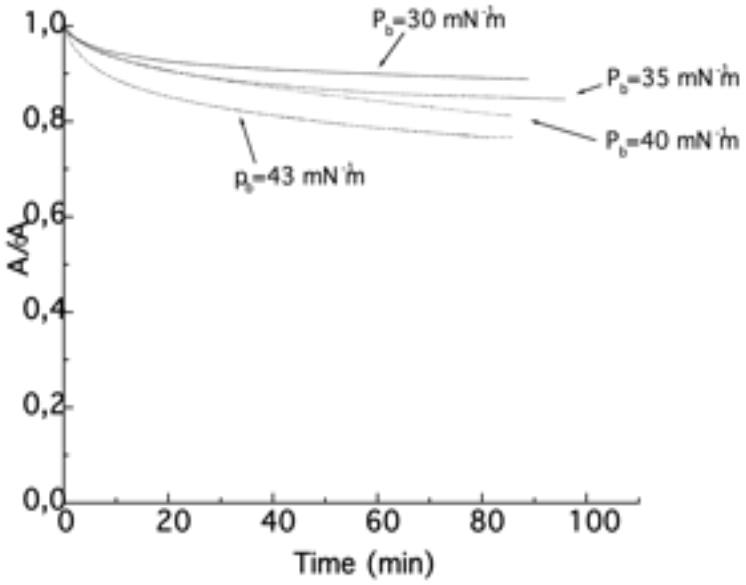

Figure 3.

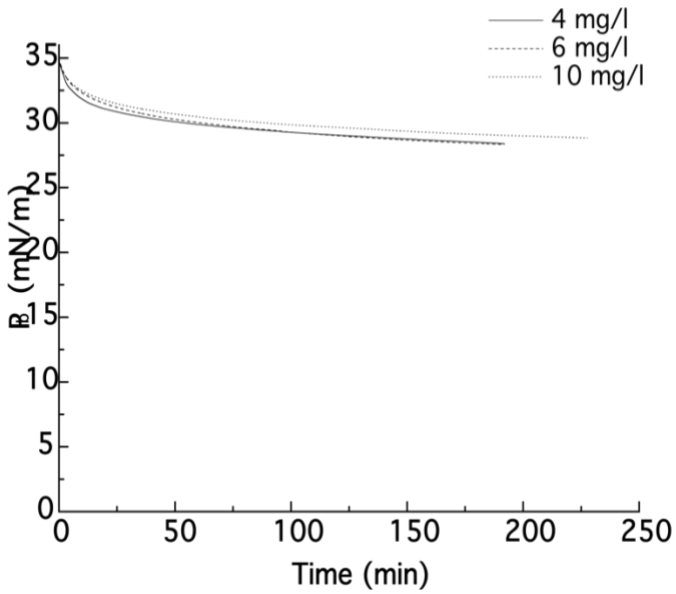

Figure 4.

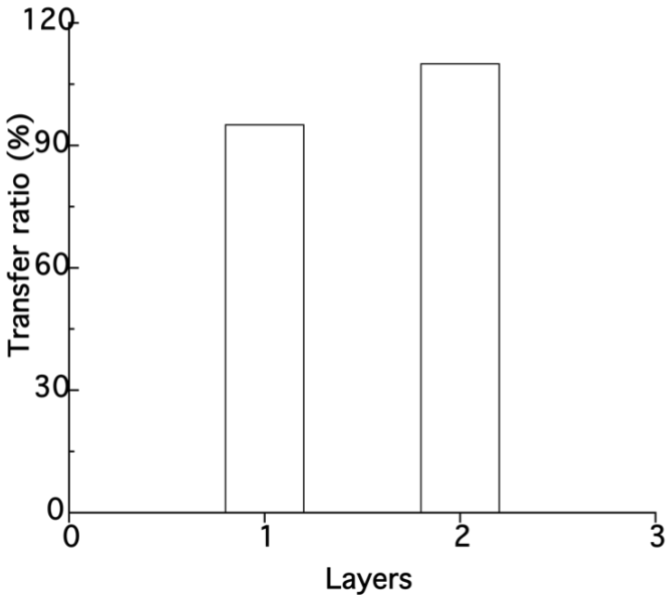

Figure 5.

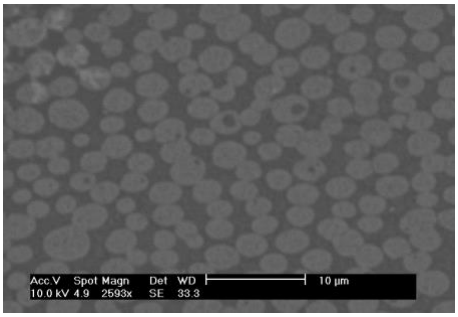

(a) P_b=30 mN m^{-1}

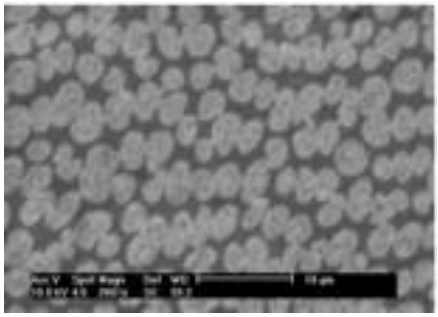

(b) P_b=35 mN m^{-1}

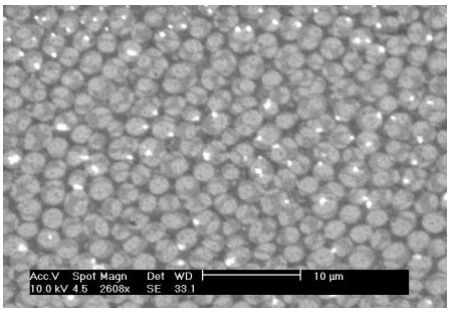

(c) P_b=40 mN m^{-1}

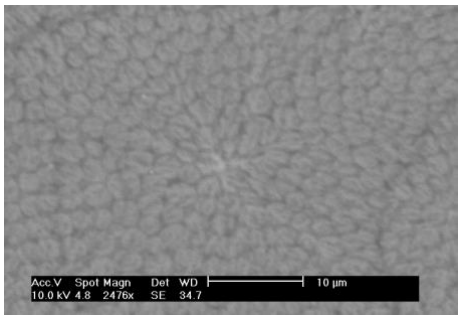

(d) P_b=43 mN m^{-1}

Figure 6.

(a)

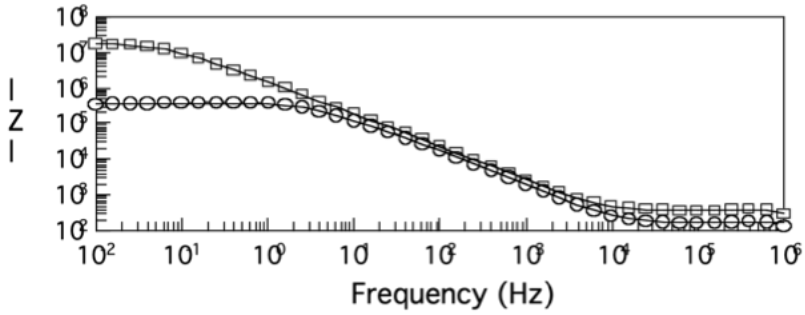

(b)

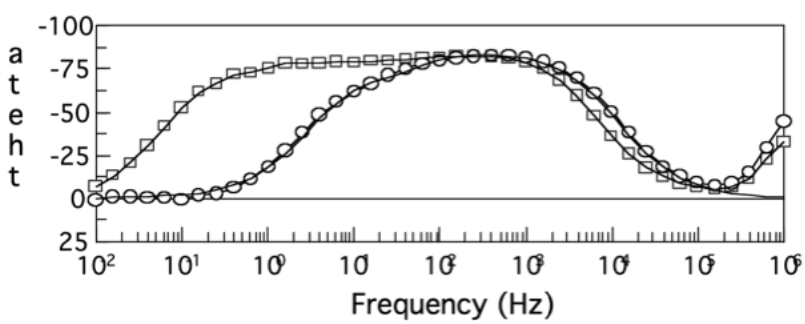

(c)

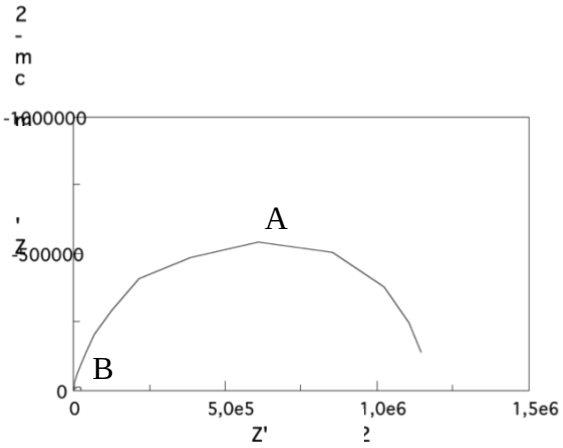

(d)

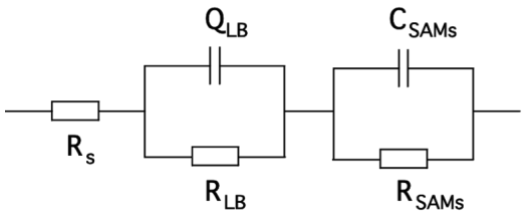

Figure 7.

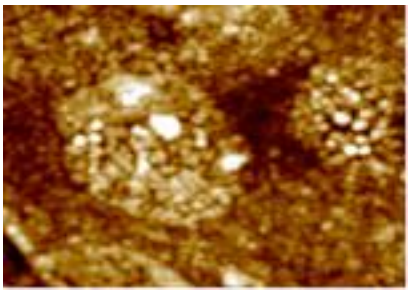

(a) topographic images

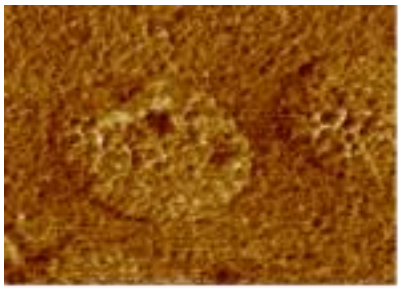

(a') phase images

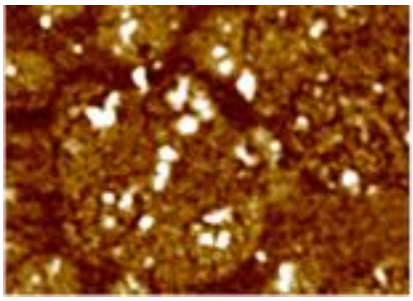

(b) topographic images

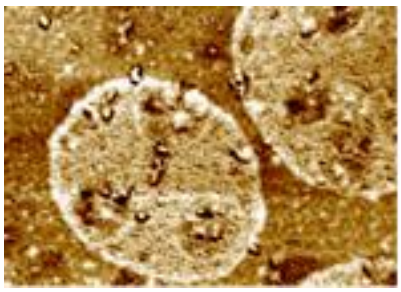

(b') Phase images

Figure 8. (need scale for the photos from Barcelona)

Table 1.

	R_S (Ω cm^2)	R_{SAMS} (Ω cm^2)	C_{SAMS} ()	R_{LB} ($M\Omega$ cm^2)	Q_{LB} ($\mu\Omega^{-1}$ cm^{-2})	n
Before odorant				1.18	1.86	0.93
After odorant				0.025	2.35	0.95